Senescent CD4 T cells Unequivocally Identify Primary Resistance and Risk of Hyperprogression to PD-L1/PD-1 Immune Checkpoint Blockade in Lung Cancer

Miren Zuazo-Ibarra[1†], Hugo Arasanz[1†], Gonzalo Fernández-Hinojal[2†], María Gato-Cañas[1†], Berta Hernández-Marín[2], Maite Martínez-Aguillo[2], Maria Jose Lecumberri[2], Angela Fernández[2], Lucía Teijeira[2], Ruth Vera[2]*, Grazyna Kochan[1]*, and David Escors[1,3]*

[1] Biomedical Research Center of Navarre-Navarrabiomed, Fundación Miguel Servet, Irunlarrea 3, 31008, Pamplona, Navarra, Spain.

[2] Department of Oncology, Hospital Complex of Navarre, Irunlarrea 3, 31008, Pamplona, Navarra, Spain.

[3] Division of Infection and Immunity, University College London, London WC1E 6JJ, United Kingdom.

*Correspondence to: Dr David Escors, d.escors@ucl.ac.uk or descorsm@navarra.es; Dr Grazyna Kochan, grazyna.kochan@navarra.es; Dr Ruth Vera, ruth.vera.garcia@navarra.es

† These authors contributed equally.

Abstract

The majority of lung cancer patients are intrinsically refractory to PD-L1/PD-1 blockade monotherapy. There is recent evidence indicating that this therapy can have serious deleterious effects by accelerating disease progression and death in a group of patients called hyperprogressors. Hence, identification of patients as hyperprogressors, non-responders and potential responders prior to therapy is of critical importance in clinical oncology. Here we demonstrate that the efficacy of PD-L1/PD-1 blockade therapy heavily relies on baseline circulating senescent CD4 T cells (Tsens). Non-small cell lung cancer (NSCLC) patients segregate in two non-overlapping groups; patients with high or with low numbers of baseline circulating Tsens. Low Tsen numbers prior to therapy unequivocally identify intrinsic non-responders, which include hyperprogressors. Additionally, unique dynamic changes in Tsens following the first cycle of therapy discriminate responders from progressors. Patients with hyperprogressive disease undergo an aberrant immunological phenomenon consisting on potent systemic proliferation of Tsens right after the first cycle of therapy (Tsen burst). ROC analysis was used to test the robustness of Tsen quantification as a predictive biomarker for primary resistance. A cut-off value of <57.7% baseline Tsens achieves 100% specificity with a 75% sensitivity for identification of primary resistance to PD-L1/PD-1 immune checkpoint blockade therapy.

Introduction

PD-L1/PD-1 blockade is demonstrating remarkable clinical outcomes since its first clinical application in human therapy (Brahmer et al., 2012; Topalian et al., 2012). These therapies interfere with immunosuppressive PD-L1/PD-1 interactions by systemic administration of blocking antibodies. PD-L1 is frequently

overexpressed by tumor cells and correlates with progression and resistance to pro-apoptotic stimuli (Azuma et al., 2008; Gato-Canas et al., 2017; Juneja et al., 2017). PD-1 is expressed in antigen-experienced T cells and interferes with T cell activation when engaged with PD-L1 (Chemnitz et al., 2004; Karwacz et al., 2011).

A significant number of lung cancer patients are intrinsically refractory to PD-L1/PD-1 immune checkpoint blockade therapies. Indeed, there is accumulating evidence that PD-L1/PD-1 blockade might even have deleterious effects by accelerating disease and death in a group of patients called hyperprogressors (Champiat et al., 2017; Saada-Bouzid et al., 2017). Currently, there is no way of identifying them before the start of therapy. Hence, stratification of patients into hyperprogressors, non-responders and potential responders is of critical importance (Topalian et al., 2016) especially when the relevance of tumor PD-L1 expression as a predictive biomarker is still under debate, at least for some cancer types (Grigg and Rizvi, 2016). Other biomarkers such as the immunoscore (Galon et al., 2006), interferon gene signatures, mutational load and microsatellite instability require relatively large biopsies (Jamieson and Maker, 2017; Vranic, 2017). These techniques are often difficult to implement in a clinical context, and the retrieval of representative biopsies can sometimes be challenging.

In addition, the impact of immunological senescence is often overlooked in cancer immunotherapies, even though most cancer patients are usually above the fifth decade of age. Human senescent T cells (Tsen cells or Tsens) accumulate with age through terminal differentiation or following prolonged antigen stimulation by a progressive loss of CD27 and CD28 expression (Lanna et al., 2014). T cells are classified as non-senescent (CD28+ CD27+), intermediately differentiated cells which lose CD27 expression and Tsens (CD28neg CD27neg) (Lanna et al., 2017; Lanna et al., 2014) **(Fig. 1A).** Although largely dysfunctional, Tsens do constitute a large pool of antigen-specific T cells with potent effector activities when mobilized (Lanna et al., 2017; Lanna et al., 2014). Indeed, PD-1 blockade can recover some effector activities of senescent CD8 T cells *in vitro* (Henson et al., 2015). However, the clinical impact of PD-L1/PD-1 immune checkpoint inhibitor therapy in Tsens and its relationship with objective clinical responses have not been addressed yet.

Here we focused on understanding the impact of Tsens over clinical responses in NSCLC patients undergoing PD-L1/PD-1 immune checkpoint blockade therapy.

Results

Baseline Tsen values separate NSCLC patients in two non-overlapping groups

Systemic circulating Tsens were quantified in a cohort of 45 NSCLC patients and healthy age-matched donors (64.8 ± 8.3 *vs* 68.60 ± 8 years old, mean±standard deviation, SD). Cancer patients showed highly significantly increased numbers of CD4 Tsens (P<0.0001) but not of CD8 Tsens. Patients were distributed in two non-overlapping groups according to CD4 Tsen basal values **(Fig. 1B);** Patients with above-average (G1 patients, 72.2% Tsens [67.2-76.8, 95% confidence interval (C.I.), N=21]) and below-average numbers (G2 patients, 28.2% Tsens [24-32.5, 95% C.I., N=24]). Accordingly, NSCLC patients showed very significantly lower numbers of non-senescent CD4 T cells (P<0.001) **(Fig. 1B)**.

Baseline Tsen numbers discriminate responses to PD-L1/PD-1 immune checkpoint blockade therapies

34 of the NSCLC patients continued with nivolumab, pembrolizumab or atezolizumab following their current indications, and at the end of the study responders accounted to 20% (7 out of 34),

consistent with the published efficacies for these agents (Herbst et al., 2016; Horn et al., 2017; Rittmeyer et al., 2017). Strikingly, CD4 Tsen values before the start of therapy unequivocally discriminated patients according to responses (P=0.0008) **(Fig. 1B and 1C).** Patients with Tsen values below 40% were all progressors [19 patients with 26.9% ± 7.8 baseline Tsens, (23-30.8, 95% C.I.)], while responders accounted to 47% of patients with Tsen values above 40% [7 out of 15 patients with 71.5% ± 9 baseline Tsens, (63-80, 95% C.I.)]. Reciprocally, patients with non-senescent CD4 T cells above 40% were all progressors **(Fig. 1D)** (P=0.005). Therefore, we defined patients with a "positive" baseline profile as those belonging to G1, while G2 represented patients with a "negative" baseline profile. PD-L1 tumor expression levels could be evaluated in 21 of the patients before therapy, and did not significantly correlate with baseline Tsen profiles (P=0.1). PD-L1 expression correlated with objective responses at the limit of statistical significance in our cohort study (P=0.052 by Fisher´s exact test) **(data not shown).**

Immune checkpoint blockade therapy induces unique dynamic changes in circulating CD4 Tsens that correlate with clinical responses

Immune checkpoint inhibitors strongly modulated CD4 T cell populations within the first cycle of treatment, and two main distinct dynamic profiles were identified. Pattern 1 or "Tsen burst" consisted in a highly significant increase in systemic CD4 Tsens [12.4% increase, (6.2, 18.5) 95% CI, N=27, P<0.0001, one-tailed paired t test)] and was associated to progressors without exception in our cohort of patients **(Fig. 2A, 2C, 2D)**. Pattern 2 or Tsen decrease was characterized by very significant reduction in systemic Tsens [-14.4%, (-8, -21), 95% CI, N=7, P<0.0001], concomitant to an expansion of non-senescent T cells and primarily associated to tumor regression **(Fig. 2B, 2C, 2D)**. There was a very highly significant correlation (P=0.0001) between Tsen changes and therapeutic outcome **(Fig. 2D)**.

To detect specific changes in CD4 T cell populations according to effector phenotypes that could be missed through conventional flow cytometry, we performed high-dimensional SPADE analyses using size, complexity, CD4, CD28 and CD27 expression as clustering parameters. Then, we analyzed the distribution of CD62L and CD45RA expression in T cell clusters to identify naïve- T stem cells ($CD45RA^{+}$ $CD62L^{+}$), central memory ($CD45RA^{neg}$ $CD62L^{+}$), effector memory ($CD45RA^{neg}$ $CD62L^{neg}$) and effector ($CD62L^{low}$ $CD45RA^{+}$) T cells. No specific clusters of CD45RA and CD62L expression profiles were observed in baseline CD4 T cells **(Fig. 3A).** Interestingly, the contraction of the Tsen population observed in responders was concomitant to an expansion of the non-senescent subset which included homogeneous clusters of effector and effector memory T cells **(Fig. 3B)** after two cycles of therapy. After four cycles of therapy, responder patients developed specific populations in the expanded non-senescent CD4 T cells with naïve-stem cell and central memory phenotypes **(Fig. 3C).** These response patterns were absent in non-responders (not shown), and suggested that contraction of the Tsen population in responders was accompanied by expansion of specific populations of non-senescent effector T cells that further differentiated into memory subsets.

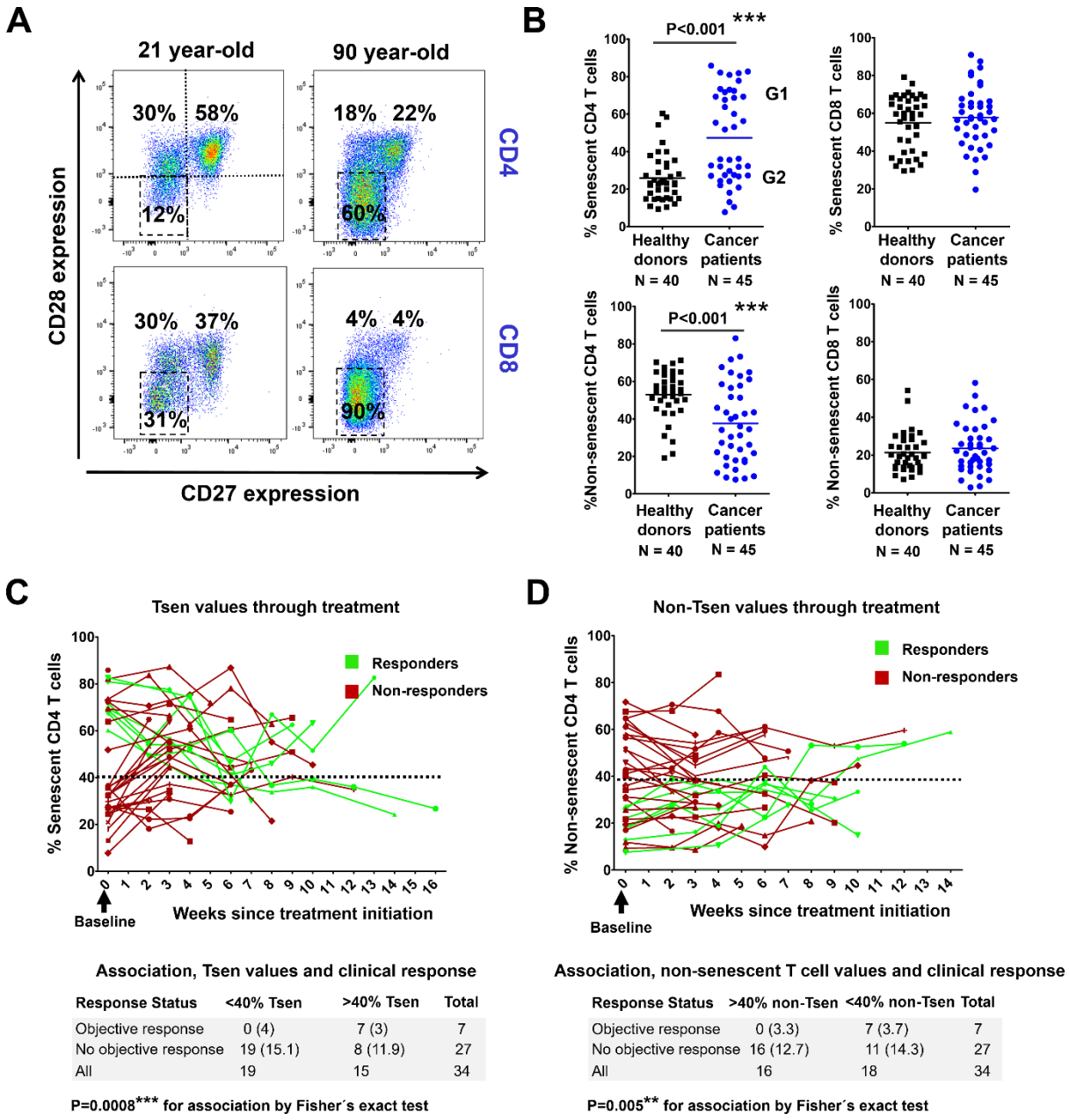

Association, Tsen values and clinical response

Response Status	<40% Tsen	>40% Tsen	Total
Objective response	0 (4)	7 (3)	7
No objective response	19 (15.1)	8 (11.9)	27
All	19	15	34

P=0.0008* for association by Fisher´s exact test**

Association, non-senescent T cell values and clinical response

Response Status	>40% non-Tsen	<40% non-Tsen	Total
Objective response	0 (3.3)	7 (3.7)	7
No objective response	16 (12.7)	11 (14.3)	27
All	16	18	34

P=0.005 for association by Fisher´s exact test**

Figure 1. Senescent T cells in NSCLC patients treated with PD-L1/PD-1 immune checkpoint inhibitors. (A) Flow cytometry density plots of CD4 (upper graphs) and CD8 T cells (lower graphs) from young (left graphs) and senior (right graphs) healthy donors, according to CD28-CD27 expression profiles. Dashed lines within the upper left graph show the gates used to quantify non-senescent (CD28+ CD27+), intermediately differentiated (CD28+ CD27neg) and Tsens (CD28neg CD27neg). Tsens are highlighted in each graph by a square. Percentages of each cell subset are indicated within the graphs. **(B)** Circulating senescent CD4 / CD8 (upper graphs), and non-senescent CD4 / CD8 (lower graphs) subsets in age-matched healthy donors or NSCLC patients before undergoing immunotherapies. G1 and G2, groups of patients classified according to high Tsens (G1) and low Tsens (G2). N, number of patients used for analyses. Relevant statistical comparisons are shown by the U of Mann-Whitney test. **(C)** Percentage of circulating Tsens in treated patients along therapy from baseline (arrow, time 0). In green, patients with objective responses. In red, non-responders. Dotted line, the lowest discriminating cut-off value (40%) separating G1 from G2 patients. No responders were observed below this cut-off value in the cohort study. Below the graph, correlation of responses to Tsen baseline values by the Fisher´s exact test. **(D)** Same as (C), but representing non-senescent T cells. **, *** indicates very and highly significant differences, respectively.

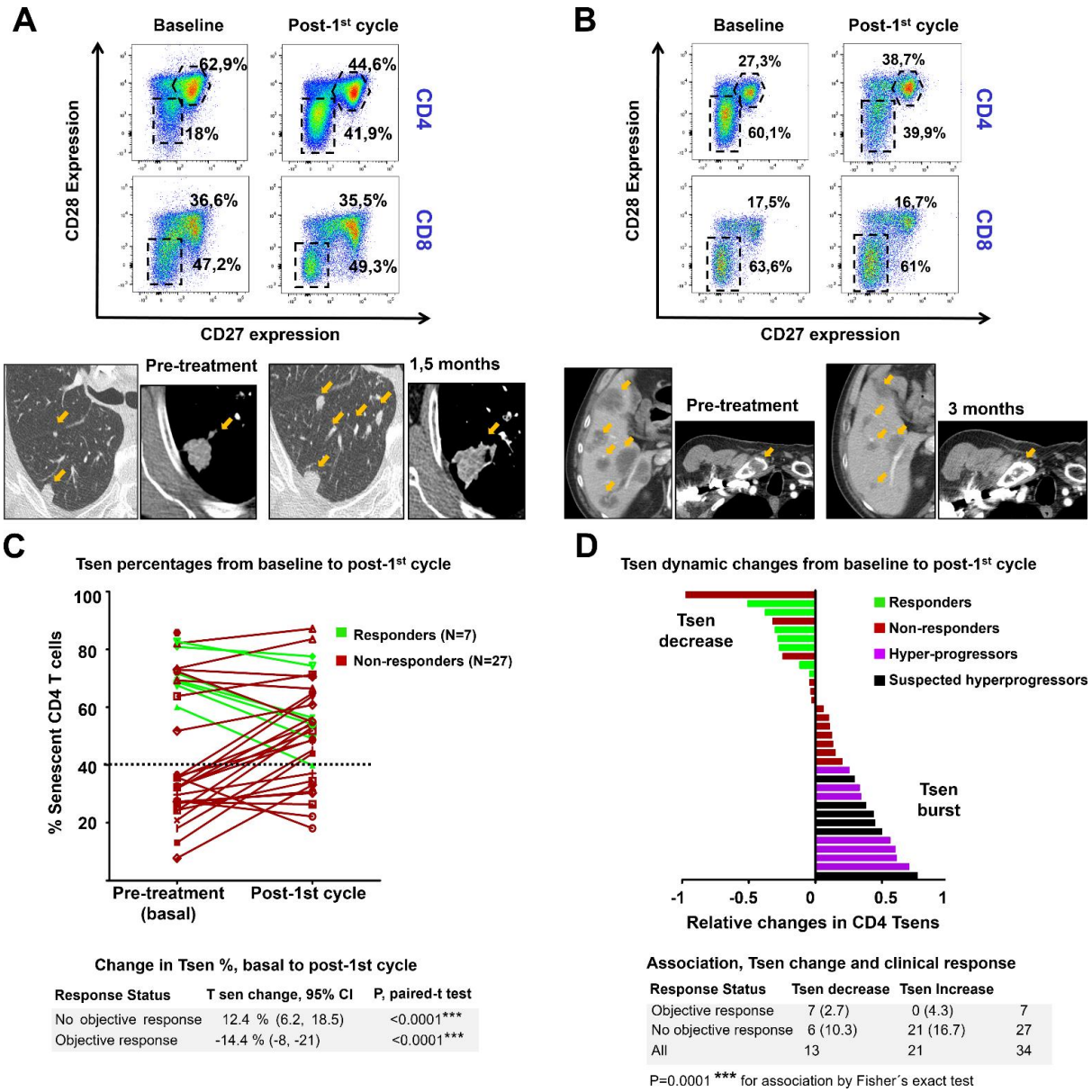

Figure 2. CD4 Tsen dynamic changes and clinical responses. (A) Clinical case of a progressor with a negative Tsen baseline profile associated to a "Tsen burst" response. Flow cytometry density plots show baseline and post-first cycle CD4 (upper graphs) and CD8 T cells (lower graphs). Senescent and non-senescent CD4 T cells are highlighted within doted boxes and hexagons, together with their percentage. Below, CT scans of lung metastases and primary tumor progressing from baseline (left scans) after one month and a half (right scans) of therapy. Lesions are indicated with arrows. **(B)** Clinical case of a responder with a positive Tsen baseline profile associated to systemic Tsen reduction. CT scans show regression of hepatic and clavicular bone metastases (indicated with arrows) before (left scans) and after 3 months (right scans) of therapy. **(C)** Change in circulating Tsens from baseline (pre-treatment) to post-first cycle of therapy. In red, progressors, in green objective responders. The 40% cut-off value is shown. Below, increase and decrease in Tsens within reponders or non-responders, as tested by one-tail paired t tests. **(D)** Waterfall plot of the relative changes in CD4 Tsens in each patient from baseline to post-first cycle of therapy. Green bars, patients with objective responses; red bars, non-responders; purple, radiologically-confirmed hyperprogressors; black, suspected hyperprogressors. Below, correlation of Tsens change with clinical outcome by the Fisher´s exact test.

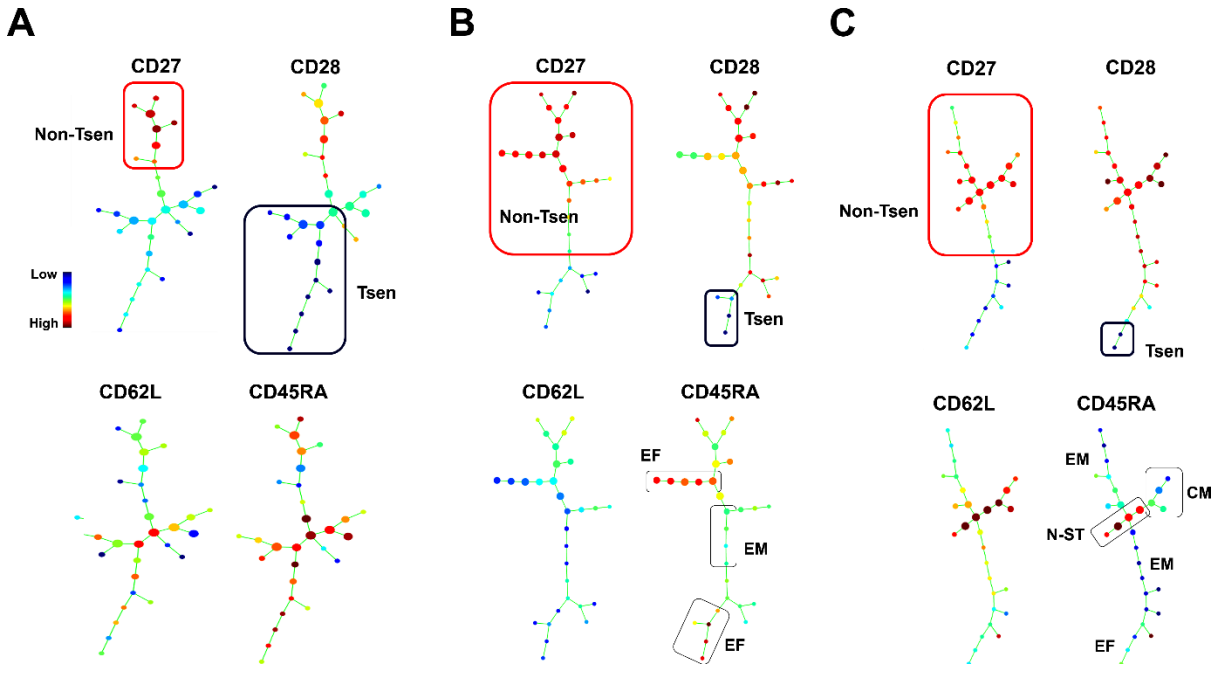

Figure 3. SPADE analyses of CD4 T cell phenotype subsets in responders through therapy. (A) SPADE high-dimensional clusters according to size, complexity, CD4, CD28 and CD27 expression are represented in CD4 T cells at baseline from a representative responder patient. The relative expression of the indicated makers is shown. Non-senescent cells are enclosed by a red rectangle, and Tsens are shown within a black rectangle. The size of clusters represent their relative frequency. **(B)** Same as in (A) but after two cycles of therapy. Clusters of effector (EF) and effector memory (EM) CD4 T cells are indicated. **(C)** Same as in (A) after four cycles of therapy. Clusters of naïve-stem (N-ST), central memory (CM), effector memory (EM) and effector T cells are indicated. The colored bar indicates the relative normalized expression levels in clusters.

CD4 Tsen bursts consist of an aberrant immunological response correlating with primary resistance to PD-L1/PD-1 blockade and hyperprogression

To find out if Tsen bursts were the result of active proliferation of CD4 Tsens from baseline to post-first cycle of therapy, Ki67 expression was analyzed by intracellular flow cytometry in Tsens from non-responder and responder patients **(Fig. 4A, 4B).** Tsens in non-responders showed a significant increase in Ki67 expression. In contrast, responders showed a markedly decrease in Tsen Ki67 expression from baseline to post-first cycle of therapy, together with increased Ki67 expression in the non-senescent CD4 T cell compartment **(Fig. 4B, 4C).** These results indicated that Tsen bursts were likely the result of systemic Tsen proliferation.

All patients with a negative baseline profile showed tumor progression **(Fig. 5A)**. Hyperprogressors were identified as defined by Sâada-Bouzid *et al* (Saada-Bouzid et al., 2017) but using as a threshold a tumor growth kinetics ratio equal or superior to 5 **(Fig. 5B)**. A negative Tsen baseline profile significantly correlated with radiologically-confirmed hyperprogressors (P=0.01) **(Fig. 5C)** whom showed highly significant Tsen bursts (P=0.0001) following the first cycle of therapy **(Fig. 5D)**. Six patients were identified as probable hyperprogressors by clinical parameters, whom either died before radiological confirmation or the disease was not evaluable by radiological criteria. Their immunological profiles were consistent with radiologically-confirmed hyperprogressors **(Fig. 5C and 5D)**. All of them experienced early progression of

disease compared to the rest (median progression-free survival (mPFS)=6 weeks [5.7-6.3, 95% C.I.] *versus* 8.9 weeks [4.6-13.1, 95% C.I.], p=0.002).
The agreement between the radiological criterium and the immunological profiling was significant in the identification of hyperprogression by a kappa test (κ=0.742). Hence, a negative baseline profile associated to significant "Tsen bursts" objectively characterized hyperprogressive disease in NSCLC patients without being influenced by previous tumor burden or dynamics.

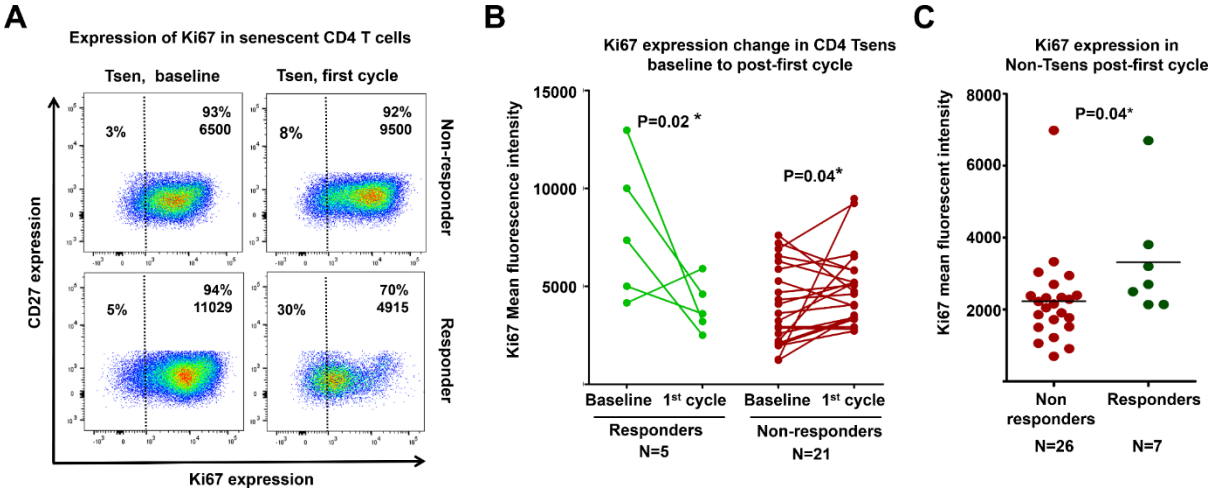

Figure 4. Proliferation of CD4 Tsens in responders and non-responders. (A) Flow cytometry density plots of Ki67 expression in Tsens from a progressor (upper two graphs) and a responder (lower two graphs) at baseline and post-first cycle of therapy as indicated. Percentage and Ki67 mean fluorescent intensities in proliferating Tsens are indicated within the graphs. **(B)** Change in Ki67 expression in Tsens from responders and non-responders as indicated. Only data was plotted in which baseline and first-cycle Ki67 values were available. Paired t-tests were performed to compare the change from baseline to post-first cycle of therapy. **(C)** Dot plots of Ki67 expression in non-senescent T cells (right graph) in non-responders and responders as indicated, in our cohort study. Expression was compared between responders and non-responders by the U of Mann-Whitney test. Relevant statistical comparisons are shown within the graphs; N, number of patients used in the analyses; **, ***, indicate very and highly significant differences.

Baseline Tsen numbers constitute a strong and reliable predictive biomarker for primary resistance and hyperprogression with practical clinical application

To improve specificity even at the cost of a lower sensitivity for identification of intrinsic non-responders, the negative baseline T cell profile was refined as the combination of Tsens <40% and non-senescent T cells > 40%. In patients with this strict negative baseline profile, the mPFS was only 6.0 weeks (95% C.I., 5.7 to 6.3) **(Fig. 6A)**. A comparison of negative and non-negative baseline profiles showed hazard ratios for disease progression or death that favored the latter [3.39 (1.4-8.17; 95% C.I.) P = 0.007] **(Fig. 6A)**. Patients were also stratified into hyperprogressors according to the immunological criteria defined in this study, with an mPFS of only 6 weeks (5.7-6.3; 95% C.I.). Hazard ratios for disease progression or death favored patients with non-hyperprogressive T cell dynamics [3.89 (1.58-9.58; 95% C.I.) P = 0.002] **(Fig. 6B).** The baseline Tsens profile was not a significant prognostic factor, as

the median time elapsed from diagnosis to enrolment for immunotherapy did not significantly differ in patients with negative or positive Tsen profiles (10.9 months vs 9.8 months, P=0.9899) (**Fig. 6C**). ROC analysis was performed in our patient cohort **(Fig. 6D)**. The association of baseline Tsens with clinical output was very significant (R=0.84, P=0.006), with a cut-off value of <57.7% to achieve 100% specificity and 75% sensitivity. These results confirmed the robustness of Tsen quantification prior to therapy as a predictive biomarker.

Discussion

Our data shows that quantification of senescent CD4 T cells from routine small blood samples provides a biomarker with strong stratification power for patients with NSCLC undergoing PD-L1/PD-1 blockade monotherapy. It allows the identification of primary resistance and risk of hyperprogressive disease in NSCLC patients before enrolment. Importantly, it is applicable to routine clinical practice. CD8 T cells were also monitored here with similar results as reported (Kamphorst et al., 2017) but without practical stratification capacities.

Responder patients presented above-average CD4 Tsen baseline numbers which may represent a pre-existing large pool of antigen-specific T cells in G1 NSCLC patients with potential anti-tumor capacities. Responders showed decreases in circulating CD4 Tsens following antibody administration, which may indicate either a recovery of CD28-CD27 expression, or mobilization from peripheral blood to secondary lymphoid organs/tumor sites. Indeed, the contraction of Tsen populations was concomitant to the expansion of non-senescent effector T cells, and the accumulation of non-senescent naïve-stem and memory CD4 T cell subsets after four cycles of therapy. This result strongly point out to a functional “CD4 reconstitution” in responders following systemic PD-L1/PD-1 blockade. In contrast, a systemic expansion of Tsens (most likely through active proliferation) was always associated to non-responders which was plainly apparent in hyperprogressors. A negative baseline profile associated to “Tsen bursts” accurately correlate with hyperprogressive disease in NSCLC without the need of obtaining radiological evidence, which supports hyperprogression as a true phenomenon with a biological basis.

According to our results in our cohort study, NSCLC patients with a negative baseline profile (G2 patients) do not respond to PD-L1/PD-1 immune checkpoint blockade monotherapy. Their identification prior to therapy helps avoiding the enrolment of hyperprogressors and intrinsic non-responders. Of the remaining patients, administration of therapy would not be indicated if Tsen bursts are observed following the first cycle of therapy. It is important to stress that Tsen numbers were stable through time in patients. This allows Tsen quantification some time before enrolment into immunotherapies without necessarily quantifying this subset right before starting therapy. Indeed, our immunological profiling helps to make objective decisions regarding NSCLC patients under PD-L1/PD-1 blockade. To translate our findings into routine clinical practice a large scale validation will be required, with a larger homogeneous target population, and the possibility of widening our study to other cancer types.

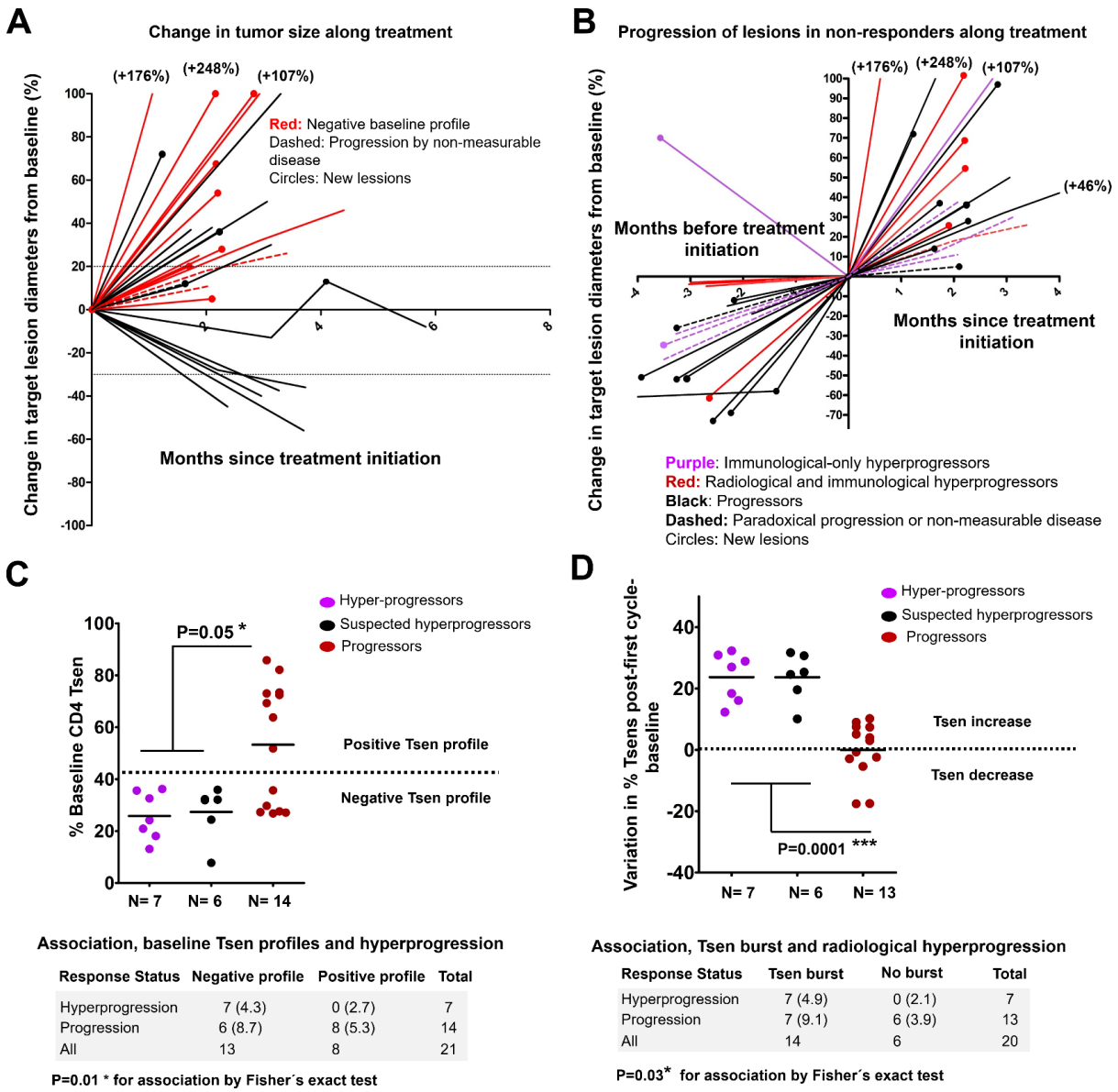

Figure 5. Tsen immunological profiles and hyperprogressive disease. (A) Spider plot of change in target lesions. Red, patients that started therapy with a negative baseline profile. These patients presented progressive disease, or growth of lesions. **(B)** Spider plot of change in target lesions of progressors before and after the start of immunotherapy. **(C)** Scatter plot of baseline Tsen values in hyperprogressors, suspected hyperprogressors and progressors, as indicated. Dotted line shows the 40% Tsens cut-off value. Below, correlation of baseline Tsens with radiologically-confirmed hyperprogressors by a Fisher´s exact test. Suspected hyperprogressors were excluded. **(D)** Scatter plot of changes in CD4 Tsen percentage from baseline to post-first cycle of therapy in radiologically-confirmed hyperprogressors, suspected hyperprogressors and progressors. Dotted line separates Tsen increases from decreases. Differences were tested by U of Mann-Whitney test. Suspected hyperprogressors were excluded. Below, correlation of Tsen burst with radiologically-confirmed hyperprogressors by a Fisher´s exact test. Probable hyperprogressors were excluded. N, number of patients in each group; Comparisons of CD4 Tsens and changes in CD4 Tsens were performed with the U of Mann-Whitney excluding suspected hyperprogressors; N, number of patients used in the analyses; *,**, ** indicates significant, very and highly significant differences.

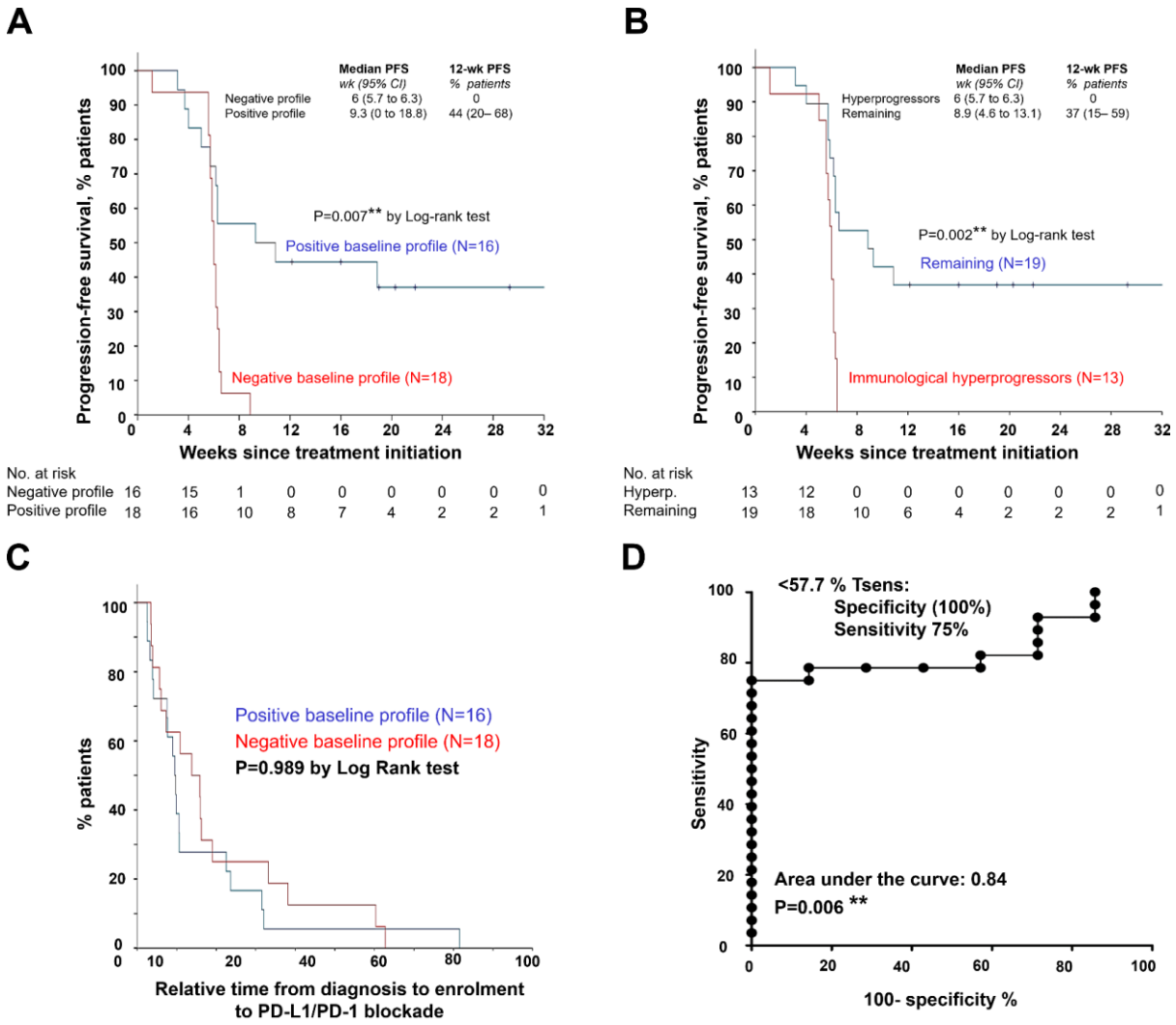

Figure 6. Survival of patients and Tsens as biomakers. (A) Kaplan-Meier plot for PFS in patients undergoing immune checkpoint inhibitor therapies stratified by strict baseline negative and positive T cell profiles as defined in the text. Patients starting therapy with a negative baseline profile had an overall response rate (ORR) of 0% and all experienced progression or death by week 9. ORR was 38.9% for patients with a positive baseline profile, and the 12-week PFS was 44%. **(B)** As in (A) but stratifying patients according to hyperprogression assessed by immunological criteria (negative Tsens baseline profile-significant Tsens burst). Patients classified as immunological progressors progressed or died by week 7. **(C)** Kaplan-Meier plot of time of diagnosis to enrolment in patients stratified by positive or negative Tsen profiles as indicated, demonstrating no significant prognostic value. **(D)** ROC analysis of baseline Tsen percentage as a predictive biomarker. Within the graph, highest Tsen cut-off value to discriminate intrinsic responders with 100% specificity. **, indicates very significant differences.

Materials and Methods

Study Design

27 patients diagnosed with non-squamous and 7 with squamous NSCLC were recruited at the Hospital Complex of Navarre **(Table S1 in supplementary material)**. Patients had all progressed to first line chemotherapy or concurrent chemo-radiotherapy. Tumor PD-L1 expression could be quantified in 21 of these patients before the start of therapies. The study was approved by the Ethics

Committee at the Hospital Complex of Navarre, and strictly followed the principles of the Declaration of Helsinki and Good Clinical Practice guidelines. A prospective study was conducted involving patients with advanced NSCLC treated with PD-L1/PD-1 immune checkpoint inhibitors (nivolumab, pembrolizumab, atezolizumab) following their current indications (Herbst et al., 2016; Horn et al., 2017; Rittmeyer et al., 2017). The mode of action, pharmacokinetics, adverse events and efficacies of the three PD-L1/PD-1 blocking agents are comparable in NSCLC, which act through the interference with the inhibitory interaction between PD-L1 and PD-1 (Herbst et al., 2016; Horn et al., 2017; Rittmeyer et al., 2017). The study was approved by the Ethics Committee at the Hospital Complex of Navarre, and strictly followed the principles of the Declaration of Helsinki and Good Clinical Practice guidelines. Written informed consent was obtained from each participant, and samples were collected by the Blood and Tissue Bank of Navarre, Health Department of Navarre, Spain.

4 ml peripheral blood samples were obtained before and during immunotherapy before administration of each cycle of treatment. PBMCs were isolated as described (Escors et al., 2008) and T cells analysed by flow cytometry. The participation of each patient concluded when a radiological test confirmed response or progression, with the withdrawal of consent or after death of the patient. Tumor responses were evaluated according to RECIST 1.1 (Eisenhauer et al., 2009) and Immune-Related Response Criteria (Wolchok et al., 2009). Hyperprogression was identified by the criteria proposed by Saada-Bouzid *et al*. (Champiat et al., 2017; Saada-Bouzid et al., 2017)

All treated patients were used for summaries of baseline characteristics and results. Objective responses were confirmed by at least one sequential tumor assessment.

Patients and healthy donors

Eligible patients were 18 years of age or older who agreed to receive immunotherapy targeting PD-1/PD-L1 following the current indications **(table S1)**. PD-L1 tumor expression was assessed when possible, but it did not constitute an inclusion criterium. Measurable disease was not required. The exclusion criteria consisted on concomitant administration of chemotherapy or previous immunotherapy treatment. NSCLC patients had an age of 64.8 ± 8.3 (mean ± standard deviation, S.D., N=45). Age-matched healthy donors were recruited from whom written informed consent was also obtained, with an age of 68.60 ± 8 (mean ± S.D., N=40).

Flow cytometry

Surface and intracellular flow cytometry analyses were performed as described.(Gato-Canas et al., 2017; Karwacz et al., 2011) T cells were immediately isolated and stained for surface expression of CD4, CD8, CD28 and CD27. 4 ml blood samples were collected from each patient, and PBMCs isolated by FICOL gradients right after the blood extraction. PBMCs were retrieved, washed and T cells distributed into aliquots and immediately stained with the indicated antibodies in a final volume of 50 µl for 10 min in ice. Cells were washed twice with PBS, resuspended in 100 µl of PBS and directly analyzed. The following fluorochrome-conjugated antibodies were used at the indicated dilutions: CD4-FITC (clone M-T466, reference 130-080-501, Miltenyi Biotec), CD4-APC-Vio770 (clone M-T466, reference 130-100-455, Miltenyi Biotec), CD4-PECy7 (clone SK3, reference 4129769, BD Biosciences,) CD27-APC (clone M-T271, reference 130-097-922, Miltenyi Biotec), CD27-PE (clone M-T271, reference 130-093-185, Miltenyi Biotec), CD45RA-FITC (reference 130-098-183, Miltenyi Biotec), CD62L-APC (reference 130-099-252, Miltenyi Biotech), CD28-PECy7 (clone CD28.2, reference 302926, Biolegend), PD1-PE (clone

EH12.2H7, reference 339905, Biolegend), CD8-FITC (clone SDK1, reference 344703, Biolegend), CD8-APC-Cy7(clone RFT-8, reference A15448, Molecular probes by Life technologies).

Spanning-tree progression analysis of density-normalized events (SPADE)

Flow cytometry data was analyzed with SPADE v3 (Qiu et al., 2011) using forward, scatter, CD4, CD28 and CD27 expression as overlapping markers for cell clustering. Arcsinh with cofactor of 150 was used for data transformation, from a maximum of 100000 events and 30 clusters. Expression of CD45RA and CD62L were not used for clustering.

Data collection

T cell percentages were quantified from peripheral blood by flow cytometry using Flowjo analysis software (Lanna et al., 2017; Lanna et al., 2014). 100000 events were recorded and the percentage of CD4/CD8 Tsens (CD28 and CD27 double-negative) and non-senescent (CD28 CD27 double-positive) were quantified prior to therapy (baseline), and before administration of each cycle of therapy. Gates in flow cytometry density plots were established taking non-senescent T cells as a reference. A minimum change in percentage above ±5% in T cell populations was considered to score increase or decrease. This value was reached according to preliminary experiments with healthy donors in which T cell numbers were monitored through several weeks. Data was recorded by M.Z.I., and separately analyzed thrice by M.Z.I. and H.A.E. independently. Cohen´s kappa coefficient was utilized to test the inter-rater agreement in classification of immunological profiles (κ=0.939).

Statistics

The mode of action, pharmacokinetics, adverse events and efficacies of the three PD-L1/PD-1 blocking agents are comparable in NSCLC (Herbst et al., 2016; Horn et al., 2017; Rittmeyer et al., 2017). Treatments administered to the patients were allocated strictly on the basis of their current indications, and independently of any variable under study. Hence, in the study design the use of all data was pre-specified to be pooled to enhance statistical power, and thereby reducing type I errors from testing the hypotheses after *had hoc* subgrouping into specific PD-L1/PD-1 blockers. The number of patients assured statistical power for Fisher´s exact test of 0.95 and superior for Student t and Mann-Whitney tests (G*Power calculator) (Faul et al., 2009), taking into account that the expected proportion of responders using any of the three PD-L1/PD-1 immune checkpoint blockade drugs in NSCLC is around 20% to 25% (if no stratification using PD-L1 tumor expression levels is used) (Herbst et al., 2016; Horn et al., 2017; Rittmeyer et al., 2017). Our study confirmed the therapeutic efficacy of these agents by achieving a 20% response rate.

Two pre-specified subgroup analyses in the study were contemplated. The first, baseline T cell values; the second, post-first cycle T cell changes from baseline. The study protocol contemplated the correlation of these values with responses using Fisher´s exact test, paired Student t tests/repeated measures ANOVA (if normally distributed) or U of Mann-Whitney/Kruskal-Wallis (if not normally distributed, or data with intrinsic high variability) to be correlated with responses. Two-tailed tests were applied with the indicated exceptions (see below). Importantly, the treatment administered to the patients was allocated independently of their basal immunological profiles, and strictly followed the current indications for the PD-L1/PD-1 inhibitors.

The percentage of T cell subsets in untreated cancer patients was normally distributed (Kolmogorov-Smirnov normality test), but not in age-matched healthy donors. Hence, to compare T cell values between two independent cancer patient groups, two-tailed unpaired Student

t tests were used while comparisons between healthy subjects and cancer patients were carried out with the U of Mann-Whitney. The mean age of cancer patients and healthy donors was 64.8 ± 8.3 (S.D.) and 68.60 ± 8 (S.D.), respectively. Percentages of T cell populations in treated patients were not normally distributed, so response groups were compared with either Mann-Whitney (comparisons between two independent groups) or Kruskall-Wallis for multi-comparison tests if required and as indicated in the manuscript. To confirm the increase or decrease in Tsens between baseline and post-first cycle of therapy in either responders or non-responders, one-tailed paired t tests were carried out. To test changes in Ki67 expression in T cells between baseline and post-first cycle of therapy in either responders or non-responders, two-tailed paired t tests were carried out. Fisher´s exact test was used to assess the association between CD4 Tsen dynamic profiles or the baseline values of Tsens with clinical responses. *Post hoc* Cohen´s kappa coefficient test was used to test the agreement of radiological versus immunological criteria for the identification of hyperprogressors.

Progression free survival (PFS) was defined as the time from the starting date of therapy to the date of disease progression or the date of death by any cause, whichever occurred first. PFS was censored on the date of the last tumor assessment demonstrating absence of progressive disease in progression-free and alive patients. PFS rates at 12 and 28-weeks was estimated as the proportion of patients who were free-of-disease progression and alive at 12 and 28 weeks after the initiation of immunotherapies. Patients who dropped out for worsening of disease and did not have a 28-week tumor assessment were considered as having progressive disease. Overall response rate (ORR) was the proportion of patients who achieved best overall response of complete or partial responses.

PFS was represented by Kaplan-Meier plots and long-rank tests utilized to compare cohorts. Hazard ratios were estimated by Cox regression models. For PFS analyses, patients were pre-specified to be stratified only on the basis of their basal Tsen values to avoid increase in type I errors due to multiplicity by subgroup analyses. Receiver operating characteristic (ROC) analysis was performed with baseline Tsen numbers and response/non-response as a binary output. Statistical tests were performed with GraphPad Prism 5 and SPSS statistical packages.

References

Azuma, T., Yao, S., Zhu, G., Flies, A. S., Flies, S. J., and Chen, L. (2008). B7-H1 is a ubiquitous antiapoptotic receptor on cancer cells. Blood *111*, 3635-3643.

Brahmer, J. R., Tykodi, S. S., Chow, L. Q., Hwu, W. J., Topalian, S. L., Hwu, P., Drake, C. G., Camacho, L. H., Kauh, J., Odunsi, K., *et al.* (2012). Safety and activity of anti-PD-L1 antibody in patients with advanced cancer. N Engl J Med *366*, 2455-2465.

Champiat, S., Dercle, L., Ammari, S., Massard, C., Hollebecque, A., Postel-Vinay, S., Chaput, N., Eggermont, A., Marabelle, A., Soria, J. C., and Ferte, C. (2017). Hyperprogressive Disease Is a New Pattern of Progression in Cancer Patients Treated by Anti-PD-1/PD-L1. Clin Cancer Res *23*, 1920-1928.

Chemnitz, J. M., Parry, R. V., Nichols, K. E., June, C. H., and Riley, J. L. (2004). SHP-1 and SHP-2 associate with immunoreceptor tyrosine-based switch motif of programmed death 1 upon primary human T cell stimulation, but only receptor ligation prevents T cell activation. J Immunol *173*, 945-954.

Eisenhauer, E. A., Therasse, P., Bogaerts, J., Schwartz, L. H., Sargent, D., Ford, R., Dancey, J., Arbuck, S., Gwyther, S., Mooney, M., *et al.* (2009). New response evaluation criteria in solid tumours: revised RECIST guideline (version 1.1). Eur J Cancer *45*, 228-247.

Escors, D., Lopes, L., Lin, R., Hiscott, J., Akira, S., Davis, R. J., and Collins, M. K. (2008). Targeting dendritic cell signalling to regulate the response to immunisation. Blood *111*, 3050-3061.

Faul, F., Erdfelder, E., Buchner, A., and Lang, A. G. (2009). Statistical power analyses using G*Power 3.1: tests for correlation and regression analyses. Behavior research methods *41*, 1149-1160.

Galon, J., Costes, A., Sanchez-Cabo, F., Kirilovsky, A., Mlecnik, B., Lagorce-Pages, C., Tosolini, M., Camus, M., Berger, A., Wind, P., *et al.* (2006). Type, density, and location of immune cells within human colorectal tumors predict clinical outcome. Science *313*, 1960-1964.

Gato-Canas, M., Zuazo, M., Arasanz, H., Ibanez-Vea, M., Lorenzo, L., Fernandez-Hinojal, G., Vera, R., Smerdou, C., Martisova, E., Arozarena, I., *et al.* (2017). PDL1 Signals through Conserved Sequence Motifs to Overcome Interferon-Mediated Cytotoxicity. Cell Rep *20*, 1818-1829.

Grigg, C., and Rizvi, N. A. (2016). PD-L1 biomarker testing for non-small cell lung cancer: truth or fiction? Journal for immunotherapy of cancer *4*, 48.

Henson, S. M., Macaulay, R., Riddell, N. E., Nunn, C. J., and Akbar, A. N. (2015). Blockade of PD-1 or p38 MAP kinase signaling enhances senescent human CD8(+) T-cell proliferation by distinct pathways. Eur J Immunol *45*, 1441-1451.

Herbst, R. S., Baas, P., Kim, D. W., Felip, E., Perez-Gracia, J. L., Han, J. Y., Molina, J., Kim, J. H., Arvis, C. D., Ahn, M. J., *et al.* (2016). Pembrolizumab versus docetaxel for previously treated, PD-L1-positive, advanced non-small-cell lung cancer (KEYNOTE-010): a randomised controlled trial. Lancet *387*, 1540-1550.

Horn, L., Spigel, D. R., Vokes, E. E., Holgado, E., Ready, N., Steins, M., Poddubskaya, E., Borghaei, H., Felip, E., Paz-Ares, L., *et al.* (2017). Nivolumab Versus Docetaxel in Previously Treated Patients With Advanced Non-Small-Cell Lung Cancer: Two-Year Outcomes From Two Randomized, Open-Label, Phase III Trials (CheckMate 017 and CheckMate 057). J Clin Oncol *35*, 3924-3933.

Jamieson, N. B., and Maker, A. V. (2017). Gene-expression profiling to predict responsiveness to immunotherapy. Cancer Gene Ther *24*, 134-140.

Juneja, V. R., McGuire, K. A., Manguso, R. T., LaFleur, M. W., Collins, N., Haining, W. N., Freeman, G. J., and Sharpe, A. H. (2017). PD-L1 on tumor cells is sufficient for immune evasion in immunogenic tumors and inhibits CD8 T cell cytotoxicity. J Exp Med *214*, 895-904.

Kamphorst, A. O., Pillai, R. N., Yang, S., Nasti, T. H., Akondy, R. S., Wieland, A., Sica, G. L., Yu, K., Koenig, L., Patel, N. T., *et al.* (2017). Proliferation of PD-1+ CD8 T cells in peripheral blood after PD-1-targeted therapy in lung cancer patients. Proceedings of the National Academy of Sciences of the United States of America *114*, 4993-4998.

Karwacz, K., Bricogne, C., Macdonald, D., Arce, F., Bennett, C. L., Collins, M., and Escors, D. (2011). PD-L1 co-stimulation contributes to ligand-induced T cell receptor down-modulation on CD8(+) T cells. EMBO Mol Med *3*, 581-592.

Lanna, A., Gomes, D. C., Muller-Durovic, B., McDonnell, T., Escors, D., Gilroy, D. W., Lee, J. H., Karin, M., and Akbar, A. N. (2017). A sestrin-dependent Erk-Jnk-p38 MAPK activation complex inhibits immunity during aging. Nat Immunol *18*, 354-363.

Lanna, A., Henson, S. M., Escors, D., and Akbar, A. N. (2014). The kinase p38 activated by the metabolic regulator AMPK and scaffold TAB1 drives the senescence of human T cells. Nat Immunol *15*, 965-972.

Qiu, P., Simonds, E. F., Bendall, S. C., Gibbs, K. D., Jr., Bruggner, R. V., Linderman, M. D., Sachs, K., Nolan, G. P., and Plevritis, S. K. (2011). Extracting a cellular hierarchy from high-dimensional cytometry data with SPADE. Nature biotechnology *29*, 886-891.

Rittmeyer, A., Barlesi, F., Waterkamp, D., Park, K., Ciardiello, F., von Pawel, J., Gadgeel, S. M., Hida, T., Kowalski, D. M., Dols, M. C., *et al.* (2017). Atezolizumab versus docetaxel in patients with previously treated non-small-cell lung cancer (OAK): a phase 3, open-label, multicentre randomised controlled trial. Lancet *389*, 255-265.

Saada-Bouzid, E., Defaucheux, C., Karabajakian, A., Coloma, V. P., Servois, V., Paoletti, X., Even, C., Fayette, J., Guigay, J., Loirat, D., *et al.* (2017). Hyperprogression during anti-PD-1/PD-L1 therapy in patients with recurrent and/or metastatic head and neck squamous cell carcinoma. Ann Oncol *28*, 1605-1611.

Topalian, S. L., Hodi, F. S., Brahmer, J. R., Gettinger, S. N., Smith, D. C., McDermott, D. F., Powderly, J. D., Carvajal, R. D., Sosman, J. A., Atkins, M. B., *et al.* (2012). Safety, activity, and immune correlates of anti-PD-1 antibody in cancer. N Engl J Med *366*, 2443-2454.

Topalian, S. L., Taube, J. M., Anders, R. A., and Pardoll, D. M. (2016). Mechanism-driven biomarkers to guide immune checkpoint blockade in cancer therapy. Nature reviews *16*, 275-287.

Vranic, S. (2017). Microsatellite instability status predicts response to anti-PD-1/PD-L1 therapy regardless the histotype: A comment on recent

advances. Bosnian journal of basic medical sciences *17*, 274-275.

Wolchok, J. D., Hoos, A., O'Day, S., Weber, J. S., Hamid, O., Lebbe, C., Maio, M., Binder, M., Bohnsack, O., Nichol, G., *et al.* (2009). Guidelines for the evaluation of immune therapy activity in solid tumors: immune-related response criteria. Clin Cancer Res *15*, 7412-7420.

Acknowledgments

We sincerely thank the patients and families that generously agreed to take part in this study.

Funding

This research was supported by Asociación Española Contra el Cáncer (AECC, PROYE16001ESCO); Instituto de Salud Carlos III, Spain (FIS project grant PI17/02119), a "Precipita" Crowdfunding grant (FECYT). D.E. is funded by a Miguel Servet Fellowship (ISC III, CP12/03114, Spain); M.Z.I. is supported by a scholarship from Universidad Pública de Navarra; H.A. is supported by a scholarship from AECC; M.G.C. is supported by a scholarship from the Government of Navarre.

Author contributions

M.Z.I. designed and carried out experiments, collected data, analyzed data. H.A.E. designed and carried out experiments, collected data, analyzed data. G.F.H. recruited patients, collected data, analyzed clinical data. M.G.C. carried out experiments, collected data, analyzed data. B.H.M. recruited patients, collected data, analyzed clinical data. M.M.A. recruited patients, collected data, analyzed clinical data. M.J.L. recruited patients, collected data, analyzed clinical data. A.F. recruited patients, collected data, analyzed clinical data. L.T. recruited patients, collected data, analyzed clinical data. R.V. supervised the clinical staff, recruited patients, analyzed clinical data. G.K. conceived the project, supervised non-clinical researchers, analysed data and wrote the paper. D.E. conceived the project, supervised non-clinical researchers, analysed data and wrote the paper. All authors participated in the writing of the manuscript.

Competing interests:

The authors declare no competing interests.

Supplementary Materials

Table S1. Baseline patient characteristics

CHARACTERISTIC	Non-Small Cell Lung Cancer (N = 34)
Age category – no. (%)	
41-50	1 (2.9%)
51-60	10 (29.4%)
61-70	15 (44.1%)
71-80	7 (20.6%)
>80	1 (2.9%)
Sex – no. (%)	
Male	25 (73.5%)
Female	9 (26.5%)
ECOG Performance-status score – no. (%)	
0-1	26 (76.5%)
2-4	8 (23.5%)
Smoking habit – no. (%)	
Yes	31 (91.2%)
No	3 (8.8%)
Metastases location – no. (%)	
Lymph nodes	3 (8.8%)
Viscera	3 (8.8%)
Both	28 (82.4%)
Immunotherapy – no. (%)	
Pembrolizumab	4 (11.8%)
Nivolumab	13 (38.2%)
Atezolizumab	17 (50%)
Treatments received during 3 months prior to immunotherapy – no. (%)	
Platinum-based chemotherapy	11 (32.3%)
Other chemotherapy	12 (35.3%)
Concurrent chemoradiotherapy	1 (2.9%)
Radiotherapy	2 (5.9%)
Targeted therapies	0 (0%)
None	8 (23.5%)
Lymphocyte count – no. (%)	
$< 1.5 \times 10^9$/L	8 (23.5%)
$1.5 – 4.0 \times 10^9$/L	26 (76.5%)
Tumor PD-L1 expression - no. (%)	
0%	9 (26.5%)
1-4%	4 (12.8%)
5-49%	4 (12.8%)
≥ 50%	5 (14.7%)

Non-evaluable	12 (35.3%)
Baseline lymphocyte profile Disfavorable Non-disfavorable	 16 (47%) 18 (53.5%)